Dynamic geometry design of cyclic peptides architectures for RNA structure

Shangbo Ning[1+], Min Sun[2+], Xu Dong[2], Anbang Li[1], Chen Zeng[3], Maili Liu[2], Zhou Gong[2]*, and Yunjie Zhao[1]*

[1]Institute of Biophysics and Department of Physics, Central China Normal University, Wuhan, 430079, China

[2]State Key Laboratory of Magnetic Resonance and Atomic Molecular Physics, Innovation Academy for Precision Measurement Science and Technology Chinese Academy of Sciences, Wuhan, Hubei 430071, China

[3]Department of Physics, The George Washington University, Washington, DC 20052, USA

[+]Contributed equally to this work.

*Correspondence:

Zhou Gong Email: gongzhou@wipm.ac.cn

Yunjie Zhao Email: yjzhaowh@mail.ccnu.edu.cn

Table S1. The docking score of top 10 peptides and SL3

Peptide	1	2	3	4	5	6	7	8	9	10	11	12	13	14	Score(*kcal/mol*)
L22	R	V	R	T	R	K	G	R	R	I	R	I	p	P	-736.50
L22#15	R	P	R	A	R	L	K	R	R	I	R	K	p	P	-816.04
L22#09	R	P	R	A	R	L	V	R	R	I	R	K	p	P	-820.39
L22#01	R	V	R	T	R	K	M	R	R	I	R	K	p	P	-827.21
L22#13	R	N	R	A	R	L	K	R	R	I	R	K	p	P	-818.02
L22#29	R	K	R	S	R	L	M	R	R	I	R	K	p	P	-811.75
L22#06	R	P	R	A	R	L	M	R	R	I	R	K	p	P	-824.70
L22#16	R	W	R	A	R	L	K	R	R	I	R	K	p	P	-816.03
L22#11	R	N	R	A	R	L	V	R	R	I	R	K	p	P	-819.71
L22#22	R	W	R	A	R	Q	M	R	R	I	R	K	p	P	-813.32
L22#43	R	P	R	S	R	L	M	R	R	I	R	K	p	P	-809.71

*D-Proline as lower-case p.

Table S2. The binding free energy (*ΔG*) of top 10 peptides and SL3 in the 50-ns MD simulation

Peptide	1	2	3	4	5	6	7	8	9	10	11	12	13	14	*ΔG (kcal/mol)*
L22	R	V	R	T	R	K	G	R	R	I	R	I	p	P	-50.08
L22#15	R	P	R	A	R	L	K	R	R	I	R	K	p	P	-121.84
L22#09	R	P	R	A	R	L	V	R	R	I	R	K	p	P	-114.48
L22#01	R	V	R	T	R	K	M	R	R	I	R	K	p	P	-102.94
L22#13	R	N	R	A	R	L	K	R	R	I	R	K	p	P	-101.45
L22#29	R	K	R	S	R	L	M	R	R	I	R	K	p	P	-98.54
L22#06	R	P	R	A	R	L	M	R	R	I	R	K	p	P	-95.18
L22#16	R	W	R	A	R	L	K	R	R	I	R	K	p	P	-93.16
L22#11	R	N	R	A	R	L	V	R	R	I	R	K	p	P	-91.59
L22#22	R	W	R	A	R	Q	M	R	R	I	R	K	p	P	-91.34
L22#43	R	P	R	S	R	L	M	R	R	I	R	K	p	P	-90.38

*D-Proline as lower-case p.

23 **Table S3. The docking score of top 10 peptides and RBE**

Peptide	1	2	3	4	5	6	7	8	9	10	11	12	13	14	Score (*kcal/mol*)
L22	R	V	R	T	R	K	G	R	R	I	R	I	p	P	-741.69
L22+16	Q	G	R	R	R	K	G	T	R	T	R	I	p	P	-879.99
L22+05	N	V	R	T	R	K	G	R	R	T	R	I	p	P	-916.36
L22+23	V	H	R	K	R	K	G	T	R	K	R	I	p	P	-874.70
L22+49	Q	G	R	R	R	K	G	C	R	T	R	I	p	P	-863.32
L22+40	V	G	R	R	R	K	G	T	R	K	R	I	p	P	-865.45
L22+34	V	W	R	Q	R	K	G	T	R	K	R	I	p	P	-867.98
L22+25	Q	G	R	R	R	K	G	A	R	T	R	I	p	P	-871.46
L22+41	Q	G	R	W	R	K	G	T	R	T	R	I	p	P	-865.29
L22+09	V	V	R	T	R	K	G	R	R	F	R	I	p	P	-887.50
L22+42	V	H	R	R	R	K	G	P	R	K	R	I	p	P	-865.20

24 **Table S4. The binding free energy (*ΔG*) of top 10 peptides and RBE in 50-ns MD**

25 **simulation**

Peptide	1	2	3	4	5	6	7	8	9	10	11	12	13	14	*ΔG (kcal/mol)*
L22	R	V	R	T	R	K	G	R	R	I	R	I	p	P	-75.02
L22+16	Q	G	R	R	R	K	G	T	R	T	R	I	p	P	-105.38
L22+05	N	V	R	T	R	K	G	R	R	T	R	I	p	P	-92.48
L22+23	V	H	R	K	R	K	G	T	R	K	R	I	p	P	-92.94
L22+49	Q	G	R	R	R	K	G	C	R	T	R	I	p	P	-93.30
L22+40	V	G	R	R	R	K	G	T	R	K	R	I	p	P	-92.31
L22+34	V	W	R	Q	R	K	G	T	R	K	R	I	p	P	-91.83
L22+25	Q	G	R	R	R	K	G	A	R	T	R	I	p	P	-89.48
L22+41	Q	G	R	W	R	K	G	T	R	T	R	I	p	P	-85.44
L22+09	V	V	R	T	R	K	G	R	R	F	R	I	p	P	-81.70
L22+42	V	H	R	R	R	K	G	P	R	K	R	I	p	P	-83.43

26 *D-Proline as lower-case p.

Table S5. The docking score (*kcal/mol*) of three cyclic peptides and four RNAs.

Cyclic peptide	TAR	SL3	RBE	PBS
L22	-612.53	-736.50	-741.69	-740.28
L22#15	-696.03	-713.44	-656.72	-709.66
L22+16	-601.71	-572.16	-710.19	-731.30

Table S6. The binding free energy (*kcal/mol*) of five 200-ns trajectories for SL3-L22#15.

Trajectory	MD01	MD02	MD02	MD04	MD05	AVE	STD
ΔG	-97.29	-86.35	-86.48	-87.26	-82.16	-87.91	5.02
TΔS	-51.27	-53.37	-50.64	-48.92	-51.02	-51.04	1.42
$\Delta G_{binding}$	-46.02	-32.98	-35.84	-38.34	-31.14	-36.86	5.19

Table S7. The binding free energy (*kcal/mol*) of five 200-ns trajectories for RBE-L22+16.

Trajectory	MD01	MD02	MD02	MD04	MD05	AVE	STD
ΔG	-83.18	-99.79	-91.12	-98.69	-84.22	-91.40	6.97
TΔS	-67.48	-66.90	-67.78	-71.16	-68.39	-68.34	1.49
$\Delta G_{binding}$	-15.70	-32.89	-23.34	-27.53	-15.83	-23.06	6.68

Table S8. The binding free energy (*kcal/mol*) of 200-ns trajectories for control.

Complex	SL3-NC	SL3-L22	RBE-RSG1.5	RBE-L22
ΔG	-63.20	-77.08	-78.26	-87.06
TΔS	-53.93	-51.81	-62.08	-71.29
$\Delta G_{binding}$	-9.27	-25.27	-16.18	-15.77

Table S9. The stereoisomers of lysine and arginine.

Name	Type	Formula	Molecular Weight	Formal Charge	2D structure	Resource References
LYS	L-type	$C_6H_{15}N_2O_2$	147.19	1		DB00123
DLY	D-type	$C_6H_{14}N_2O_2$	146.19	0		DB03252
DAB	L-type	$C_4H_{10}N_2O_2$	118.13	0		DB03817
4FO	D-type	$C_4H_{10}N_2O_2$	118.13	0		134490
ORN	L-type	$C_5H_{12}N_2O_2$	132.16	0		DB00129
ORD	D-type	$C_5H_{12}N_2O_2$	132.16	0		71082
ARG	L-type	$C_6H_{15}N_4O_2$	175.21	1		DB00125
DAR	D-type	$C_6H_{15}N_4O_2$	175.21	1		DB04027
4J5	L-type	$C_5H_{13}N_4O_2$	161.18	1		137348247
HRG	L-type	$C_7H_{16}N_4O_2$	188.23	0		DB03974

*The stereoisomers of lysine and arginine, which adopt extended, shortened, non-standard or chiral mimics, can be used to construct new peptide libraries to improve contacts with RNA. The amino acids' side chain length and chirality can be directed to make the cyclic peptide more suitable for a specific RNA pocket.

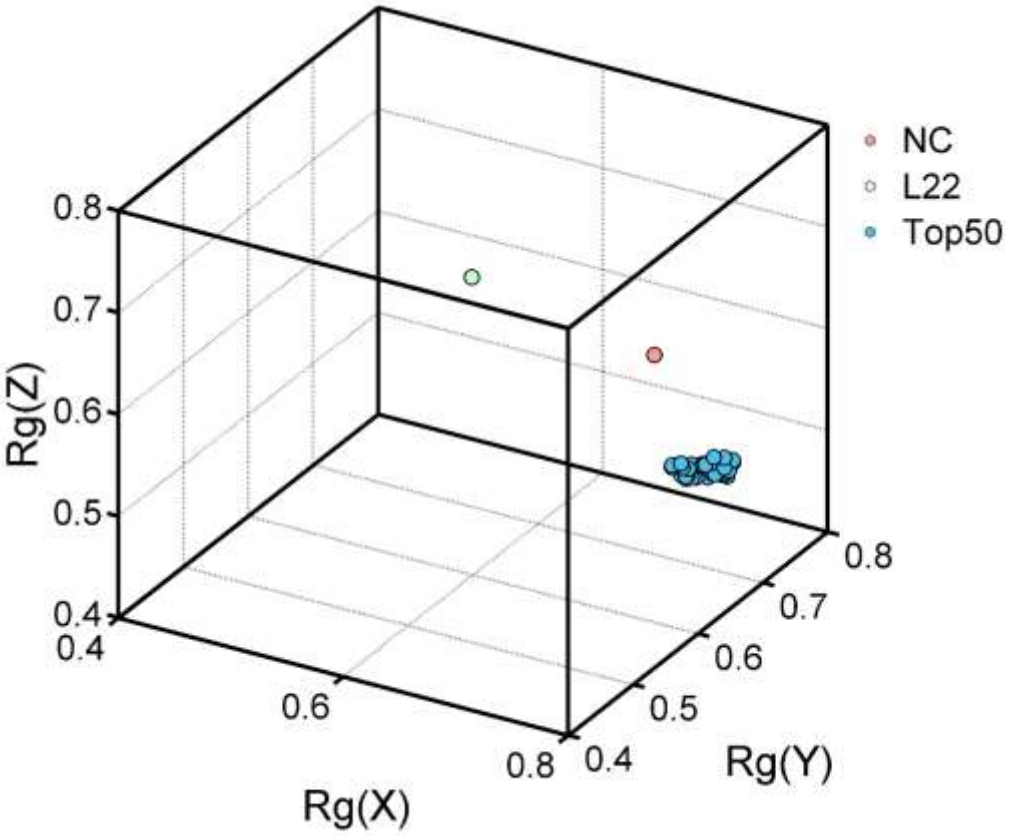

Figure S1. The radius of gyration (Rg) around the X, Y and Z axes of NC, L22 and top 50 cyclic peptides.

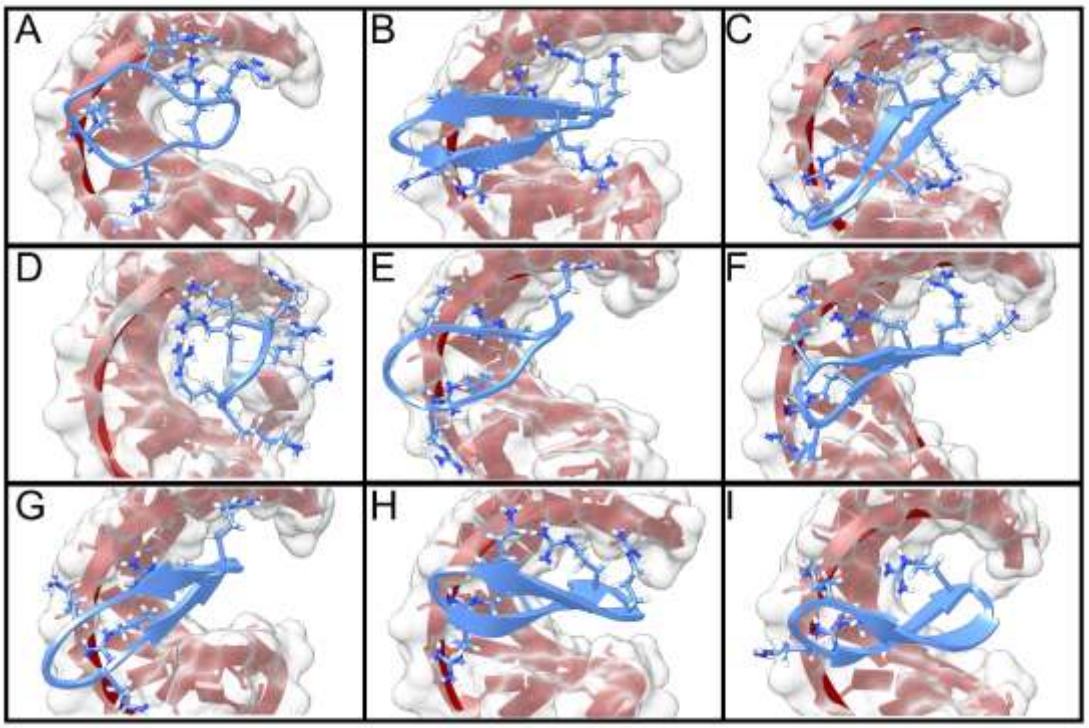

Figure S2. The interactions between SL3 and the other 9 cyclic peptides. (A). L22#09, (B) L22#01, (C) L22#13, (D) L22#29, (E) L22#06, (F) L22#16, (G) L22#11, (H) L22#22, (I) L22#43.

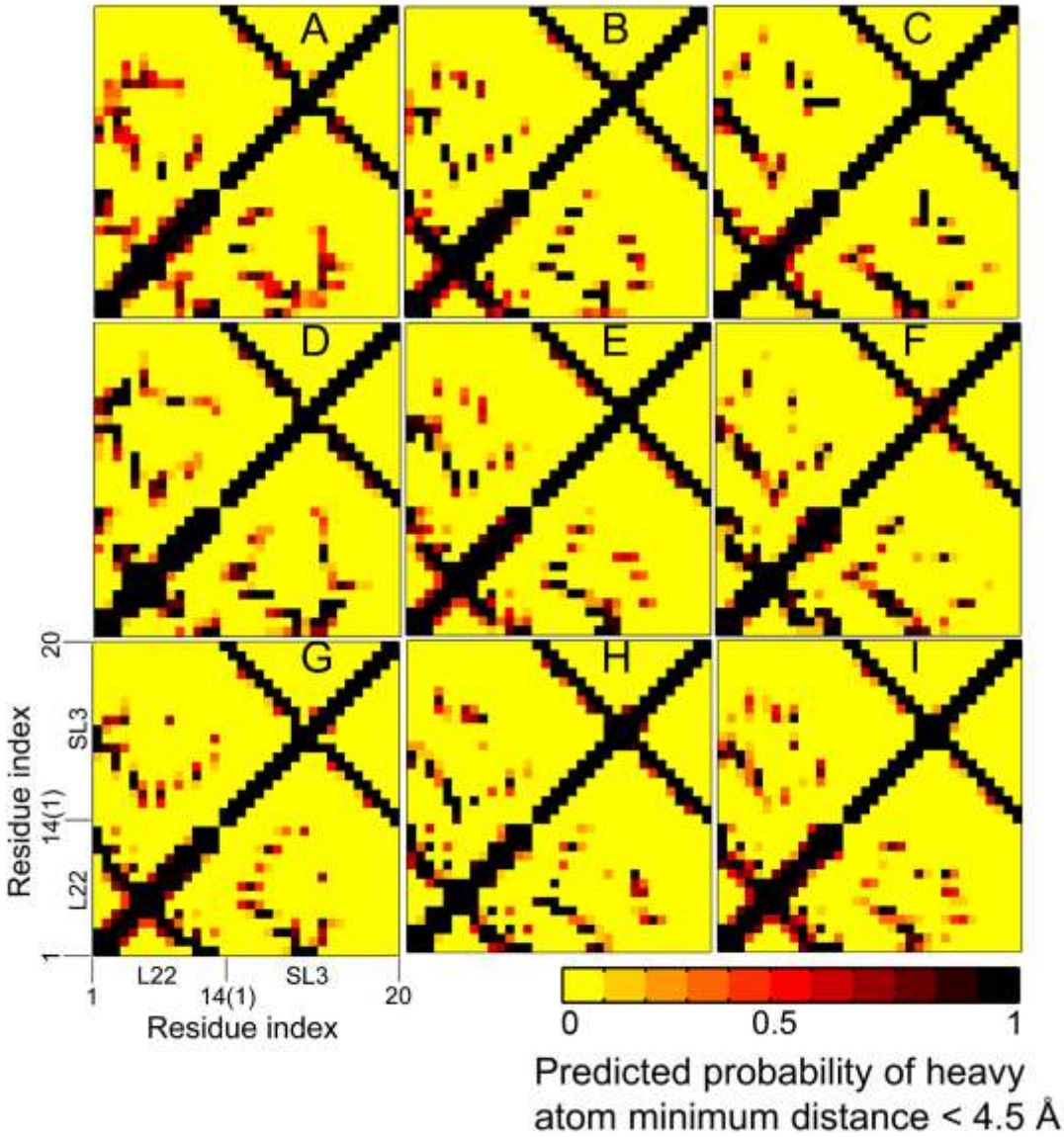

Figure S3. The contact map between SL3 and the other 9 cyclic peptides in the 50-ns MD simulation. (A). L22#09, (B) L22#01, (C) L22#13, (D) L22#29, (E) L22#06, (F) L22#16, (G) L22#11, (H) L22#22, (I) L22#43.

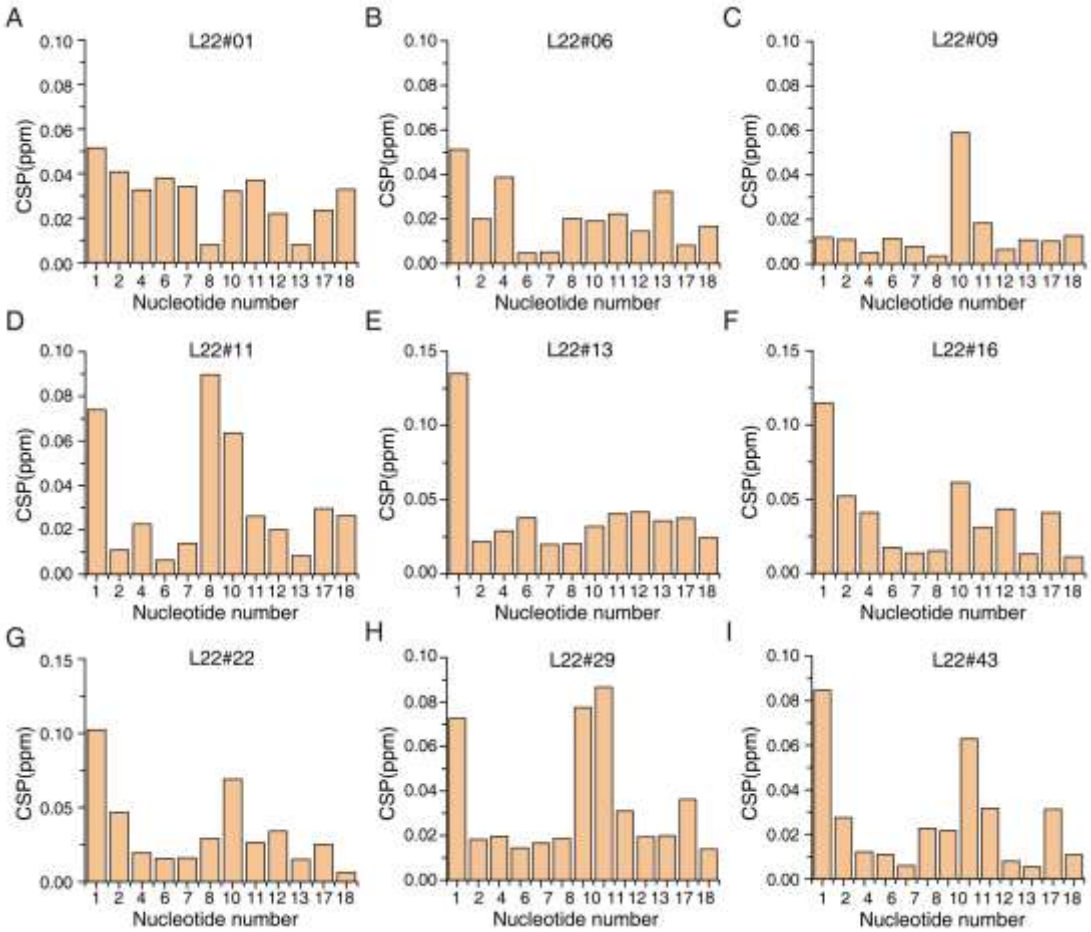

Figure S4. CSPs from titration of the other 9 peptides (400μM) into the SL3 RNA solution (200μM) under experimental conditions of NaH_2PO_4(25 mM), NaCl (100 mM), 10% D_2O and pH 6.8 at 280K. The analysis specifically examines the nucleotide signals corresponding to C8-H8 or C6-H6. The significant CSPs observed in the nucleotides indicate their potential involvement in establishing the interaction interface with SL3.

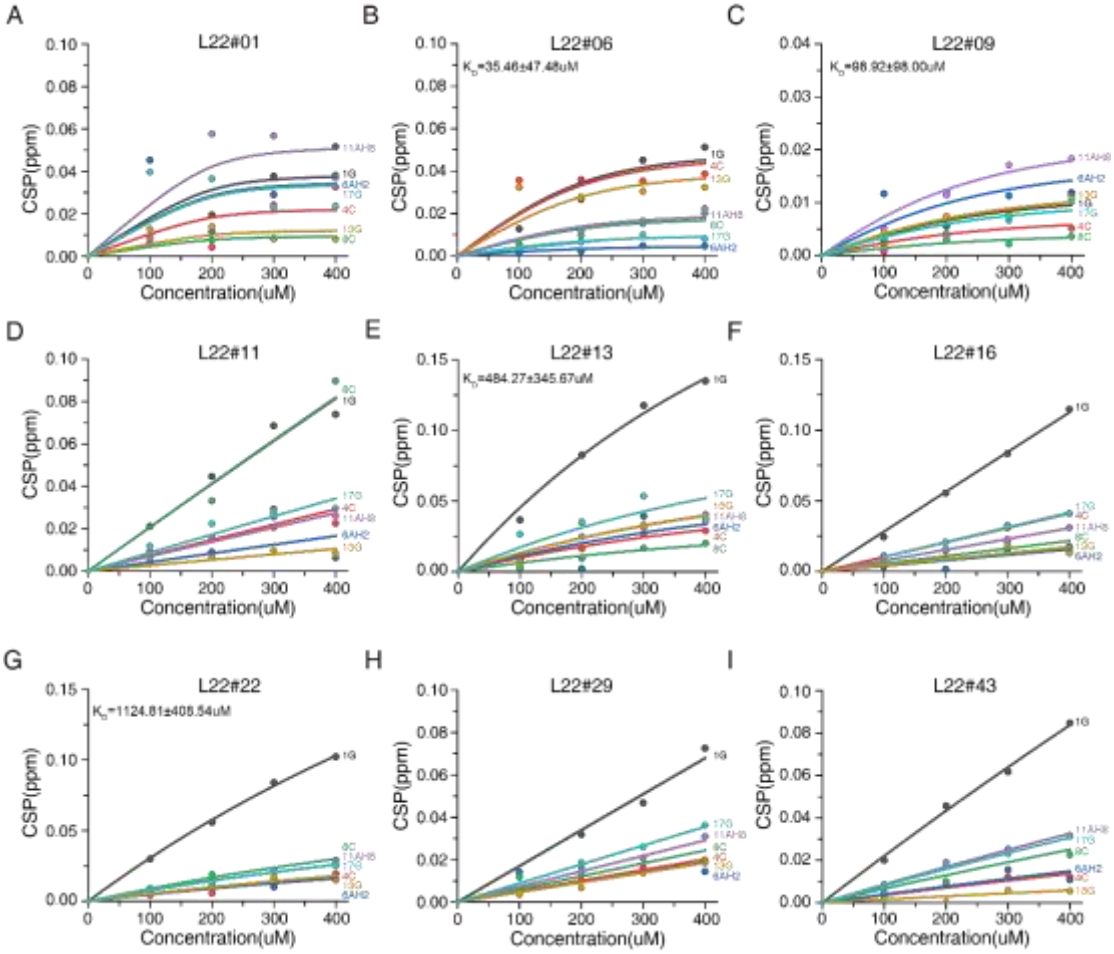

Figure S5. Global fitting of the binding equilibrium constant of the other 9 peptides to SL3 using nucleotides exhibiting significant CSPs (represented by different colors).

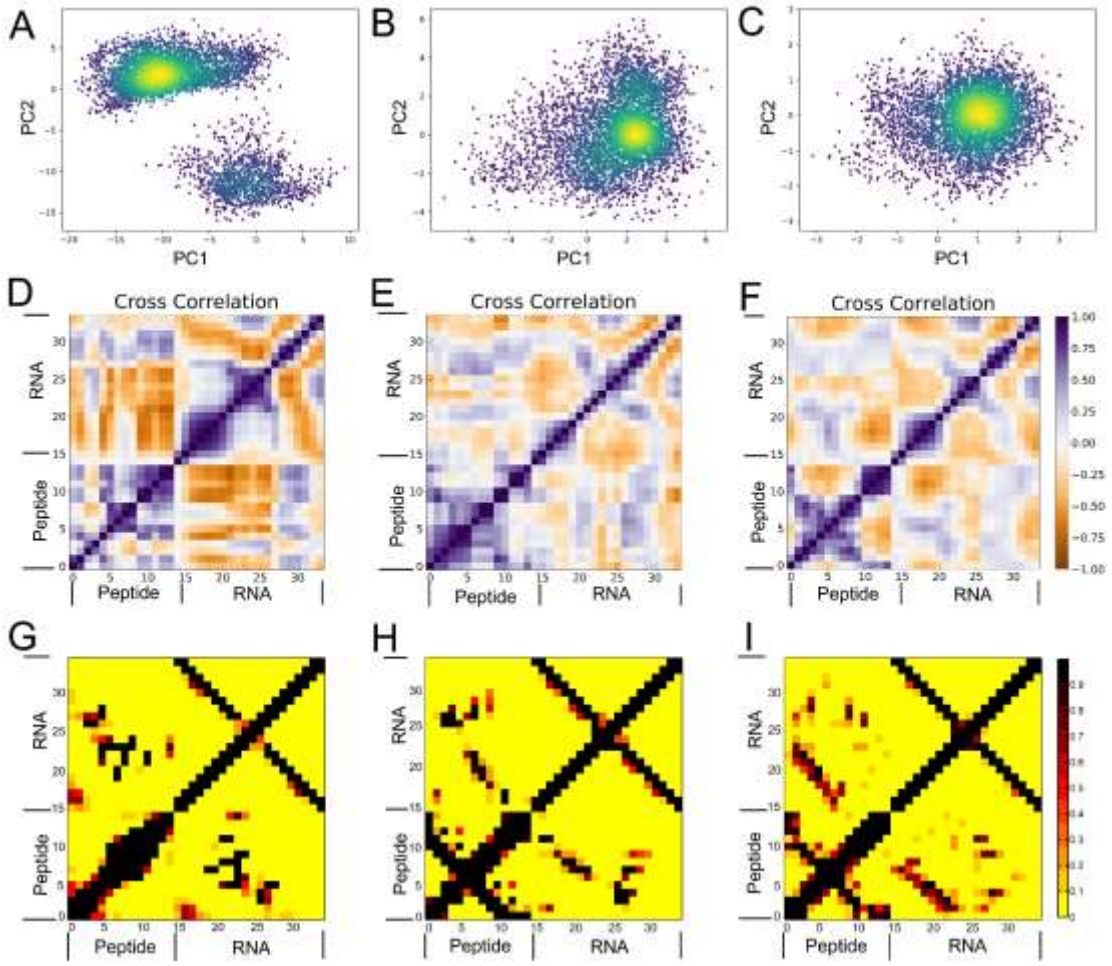

Figure S6. Different binding modes of three peptides to SL3 RNA. The principal component analysis (PCA) between SL3 and three peptides in the 200-ns MD simulation, (A) SL3-NC, (B) SL3-L22, (C) SL3-L22#15. The dynamic cross-correlation matrix (DCC) between SL3 and three peptides in the 200-ns MD simulation, (D) SL3-NC, (E) SL3-L22, (F) SL3-L22#15. The contact map between SL3 and three peptides in the 200-ns MD simulation, (G) SL3-NC, (H) SL3-L22, (I) SL3-L22#15.

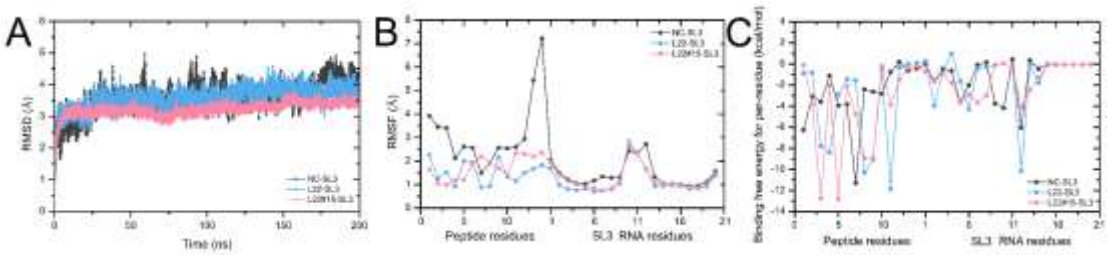

Figure S7. Dynamics fluctuation of three systems in the 200-ns MD simulation, NC-SL3, L22-SL3, and L22#15-SL3. (A) The root-mean-square deviation of the overall structure of the three complexes. (B) The root-mean-square fluctuation of per-residue of the three complexes. (C) The free energy contributes to the binding free energy of the per-residue of the three complexes.

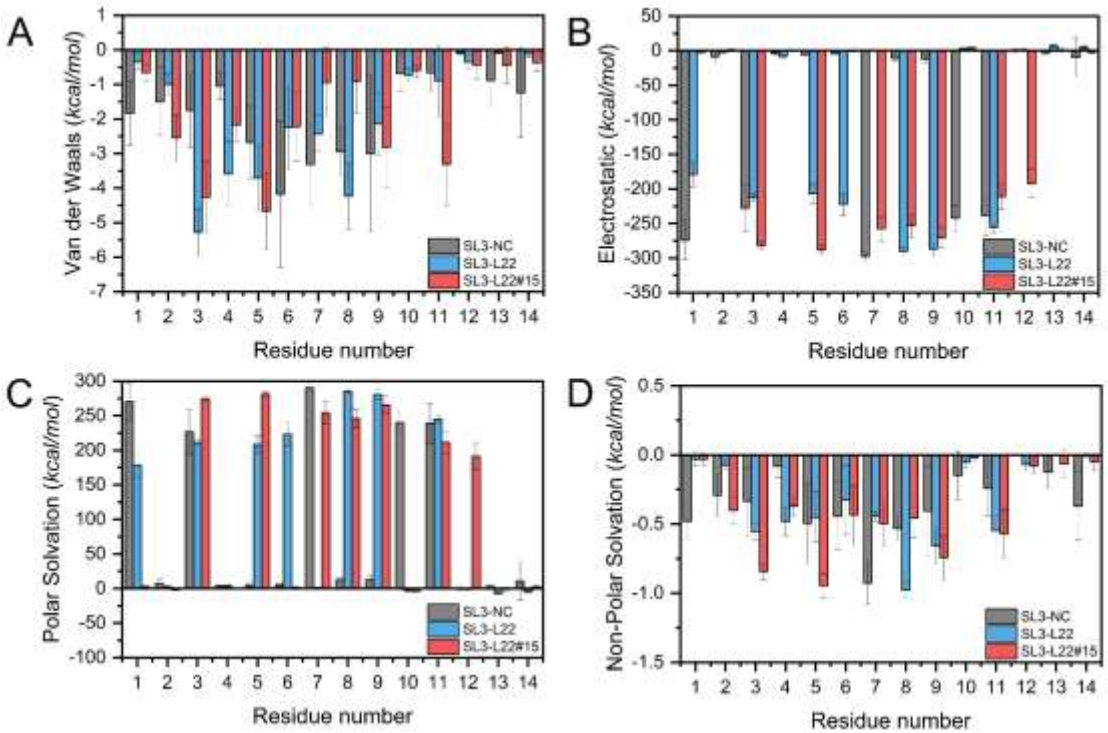

Figure S8. The free energy contribution of SL3 RNA binding to the three peptides from different interactions. (A) van der Waals, (B) electrostatic, (C) Polar Solvation, (D) Non-polar Solvation.

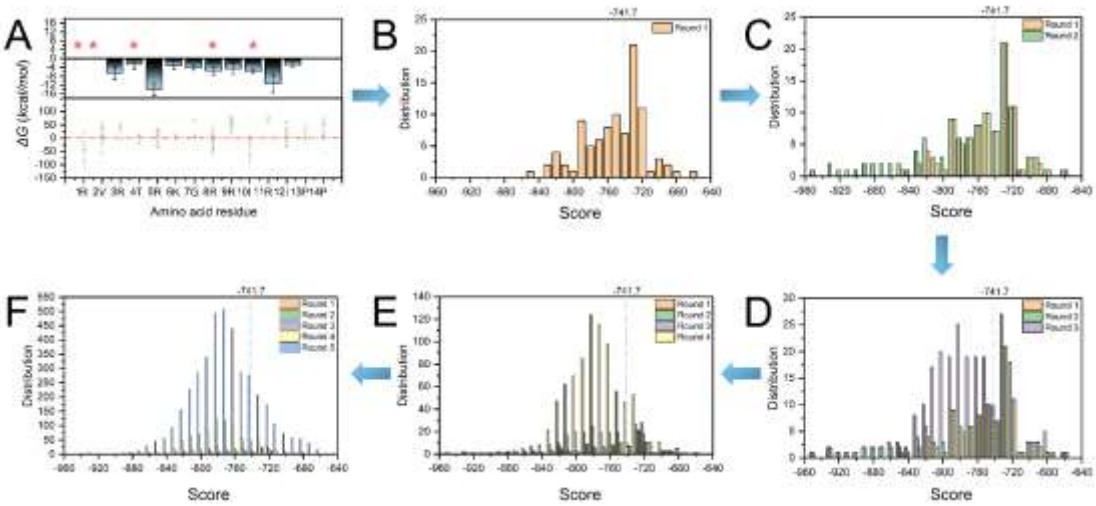

Figure S9. The top 50 inhibitors for RBE are preliminarily screened by docking and per-residue-free energy decomposition. (A) Decomposing the free energy contributions in a per-residue of L22-RBE are calculated by MM-GBSA. Single point mutations are performed for per-residue of L22. The docking scores are calculated by HDOCK. The interaction optimization for the cyclic peptides and RBE RNA is divided into five steps: (B) round 1, (C) round 2, (D) round 3, (E) round 4, (F) round 5.

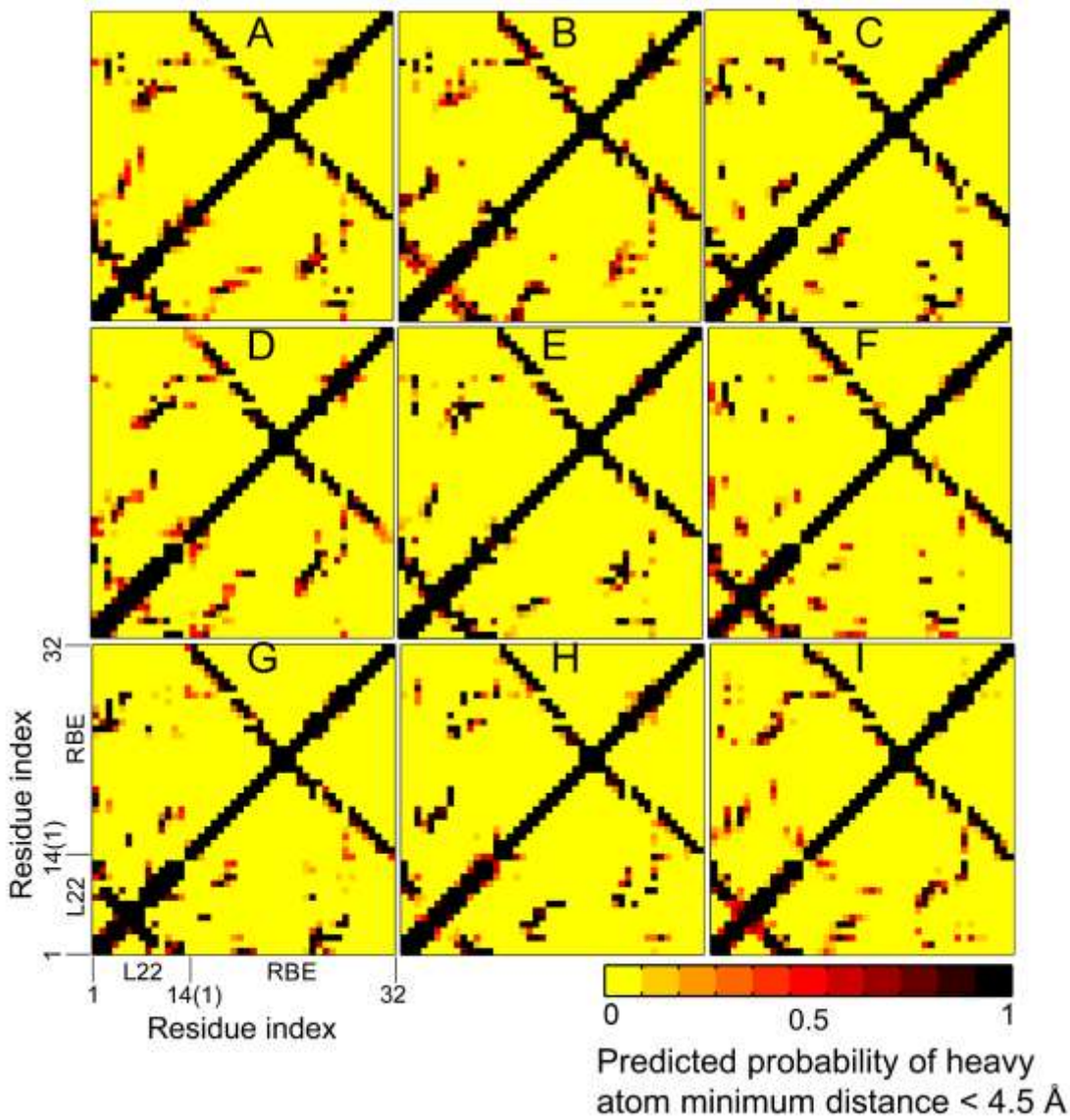

Figure S10. The contact map between RBE and the other 9 cyclic peptides in 50-ns MD simulation. (A). L22+05, (B) L22+23, (C) L22+49, (D) L22+40, (E) L22+34, (F) L22+25, (G) L22+41, (H) L22+09, (I) L22+42.

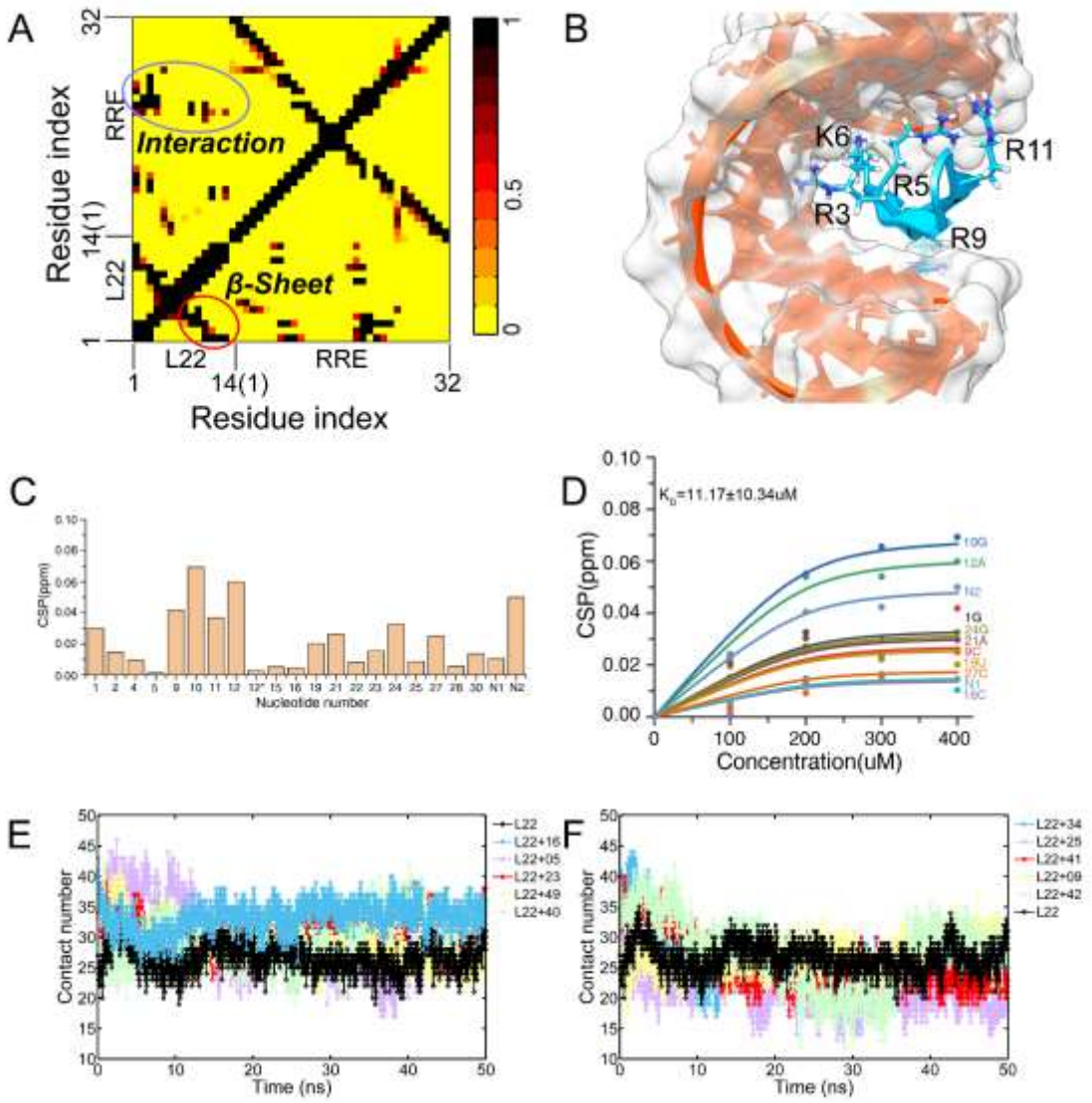

Figure S11. The binding affinity between top 1 peptide L22+16 and RBE in 50-ns MD simulation and NMR experiments. (A) The contact map shows that the interaction between L22+16 and RBE is stable and the secondary structure of cyclic peptide is still stabilized in the MD simulation. (B) The interaction surface locates at the hairpin stem-loop of RBE and the positively charged amino acids of L22+16. (C) CSPs from titration of the L22+16 (400μM) into the RBE RNA solution (200μM) under experimental conditions of NaH2PO4 (25 mM), NaCl (100 mM), 10% D2O and pH 6.8 at 298K. The analysis specifically examines the nucleotide signals corresponding to C8-H8 or C6-H6. Additionally, * represents the signal of nucleotide C2-H2. N1 and N2 mean the corresponding peaks that were not assigned. The significant CSPs observed in the nucleotides indicate their potential involvement in establishing the interaction interface with RBE RNA. (D) Global fitting of the binding equilibrium constant of L22+16 and

RBE RNA using nucleotides exhibiting significant CSPs (represented by different colors). (E). The contact number of residue-residue pairs between top 1-5 and RBE changed along with time; (F) The contact number of residue-residue pairs between top 1-5 and RBE changed along with time.

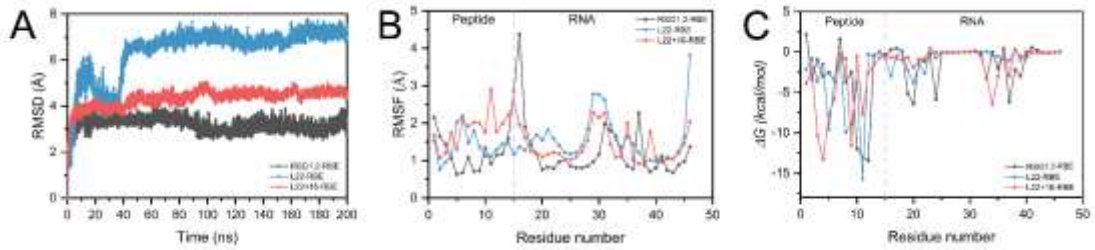

Figure S12. Dynamics fluctuation of three systems in the 200-ns MD simulation, RSG-1.2-RBE, L22-RBE, and L22+16-RBE. (A) The root-mean-square deviation of the overall structure of the three complexes. (B) The root-mean-square fluctuation of per-residue of the three complexes. (C) The free energy contributes to the binding free energy of the per-residue of the three complexes.

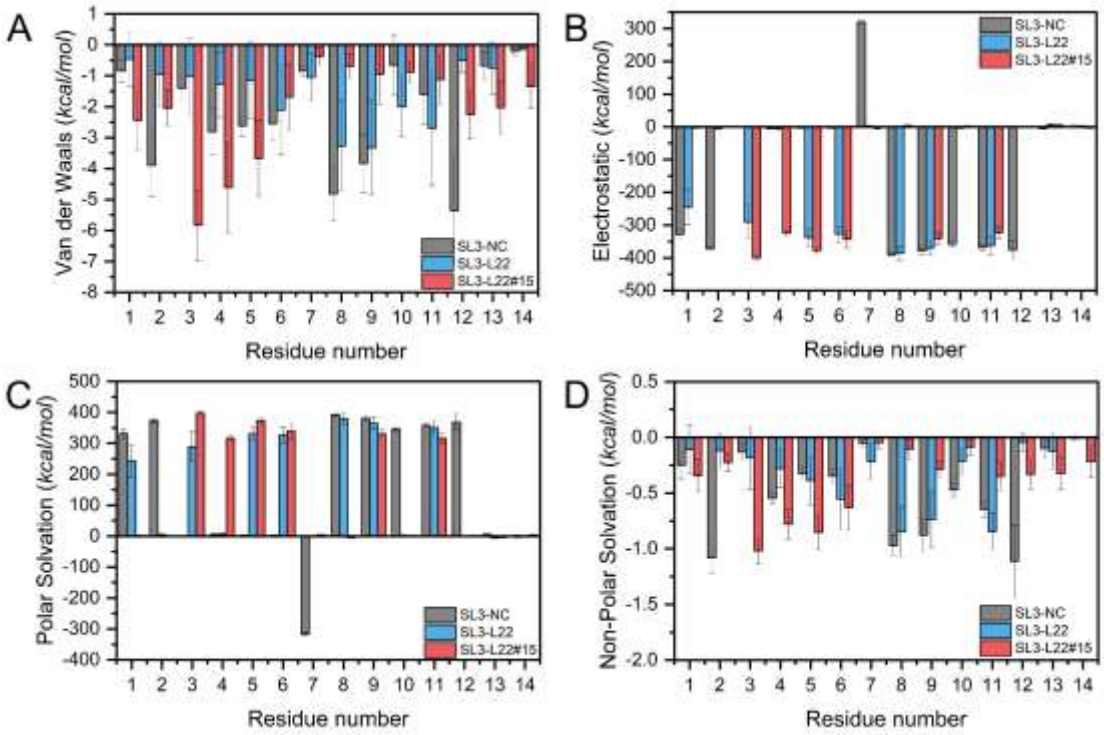

Figure S13. The free energy contribution of RBE RNA binding to the three peptides from different interactions. (A) van der Waals, (B) electrostatic, (C) Polar Solvation, (D) Non-polar Solvation.

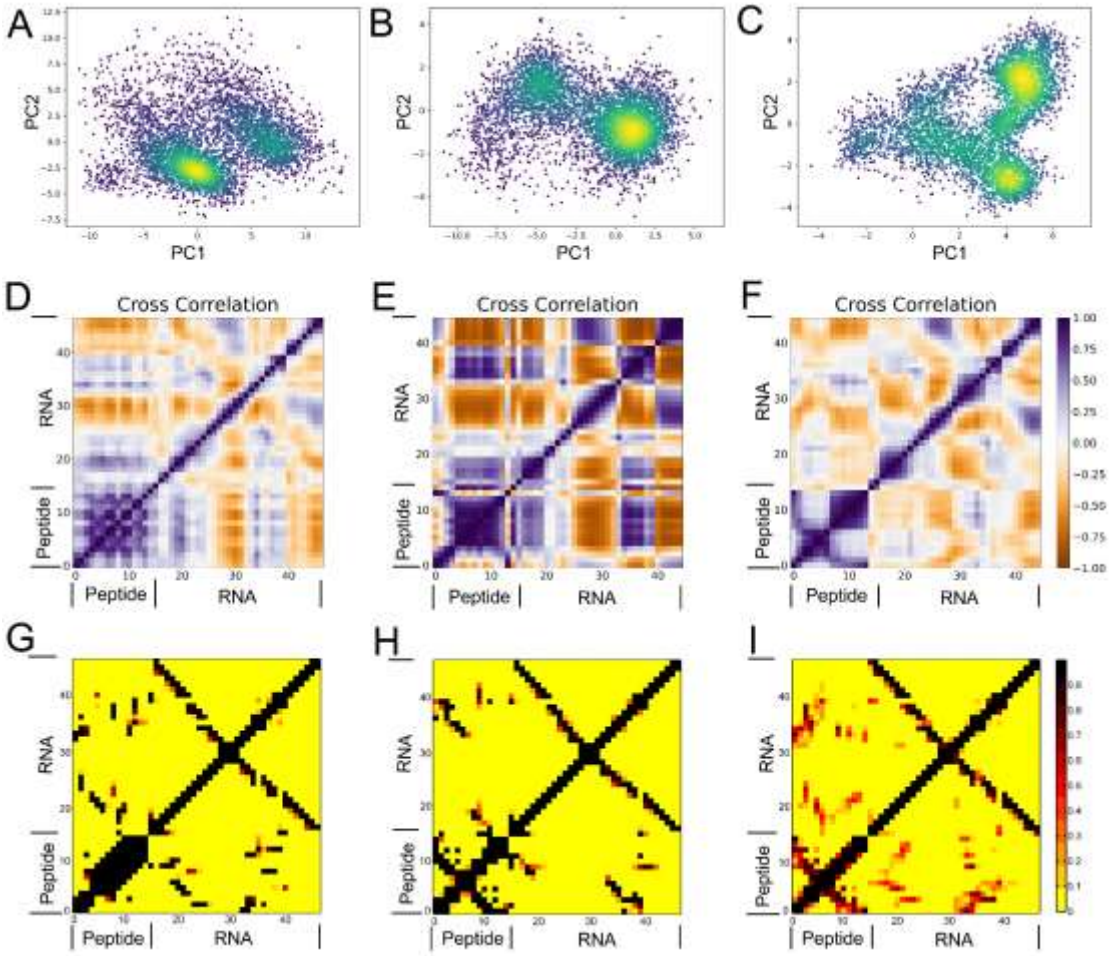

Figure S14. Different binding modes of three peptides to RBE RNA. The principal component analysis (PCA) between RBE and three peptides in the 200-ns MD simulation, (A) RBE-RSG-1.5, (B) RBE-L22, (C) RBE-L22+16. The dynamic cross-correlation matrix (DCC) between RBE and three peptides in the 200-ns MD simulation, (D) RBE-RSG-1.5, (E) RBE-L22, (F) RBE-L22+16. The contact map between RBE and three peptides in the 200-ns MD simulation, (G) RBE-RSG-1.5, (H) RBE-L22, (I) RBE-L22+16.

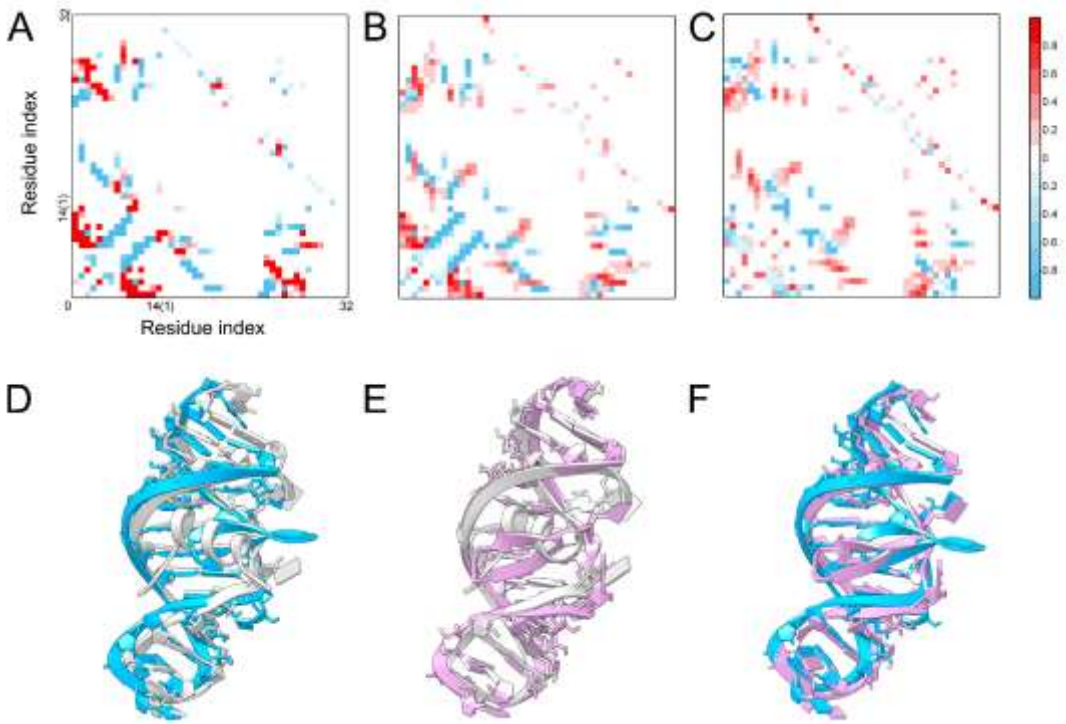

Figure S15. The comparison of binding modes between three peptides and RBE in 200-ns MD simulation. The different of contact between RBE and three peptides, (A) L22/RSG-1.2, (B) L22+16/RSG-1.2 and (C) L22+16/L22. The structural overlap corresponding to the contact map, (D) L22/RSG-1.2, (E) L22+16/RSG-1.2 and (F) L22+16/L22.

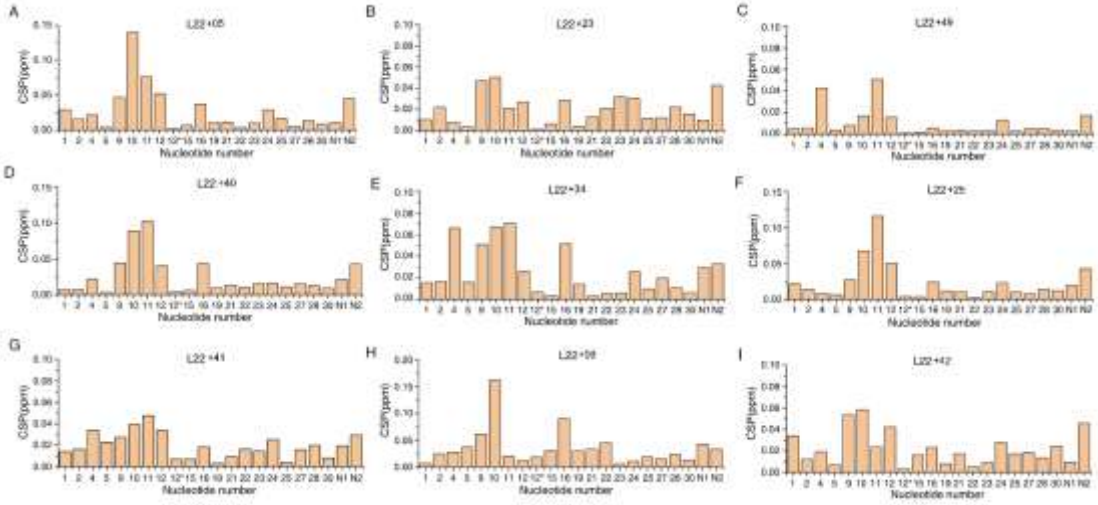

Figure S16. CSPs from titration of the other 9 peptides (400μM) into the RBE RNA solution (200μM) under experimental conditions of NaH_2PO_4(25 mM), NaCl (100 mM), 10% D_2O and pH 6.8 at 298K. The analysis specifically examines the nucleotide signals corresponding to C8-H8 or C6-H6. Additionally, * represents the signal of nucleotide C2-H2. N1 and N2 mean the corresponding peaks that were not assigned. The significant CSPs observed in the nucleotides indicate their potential involvement in establishing the interaction interface with RBE RNA.

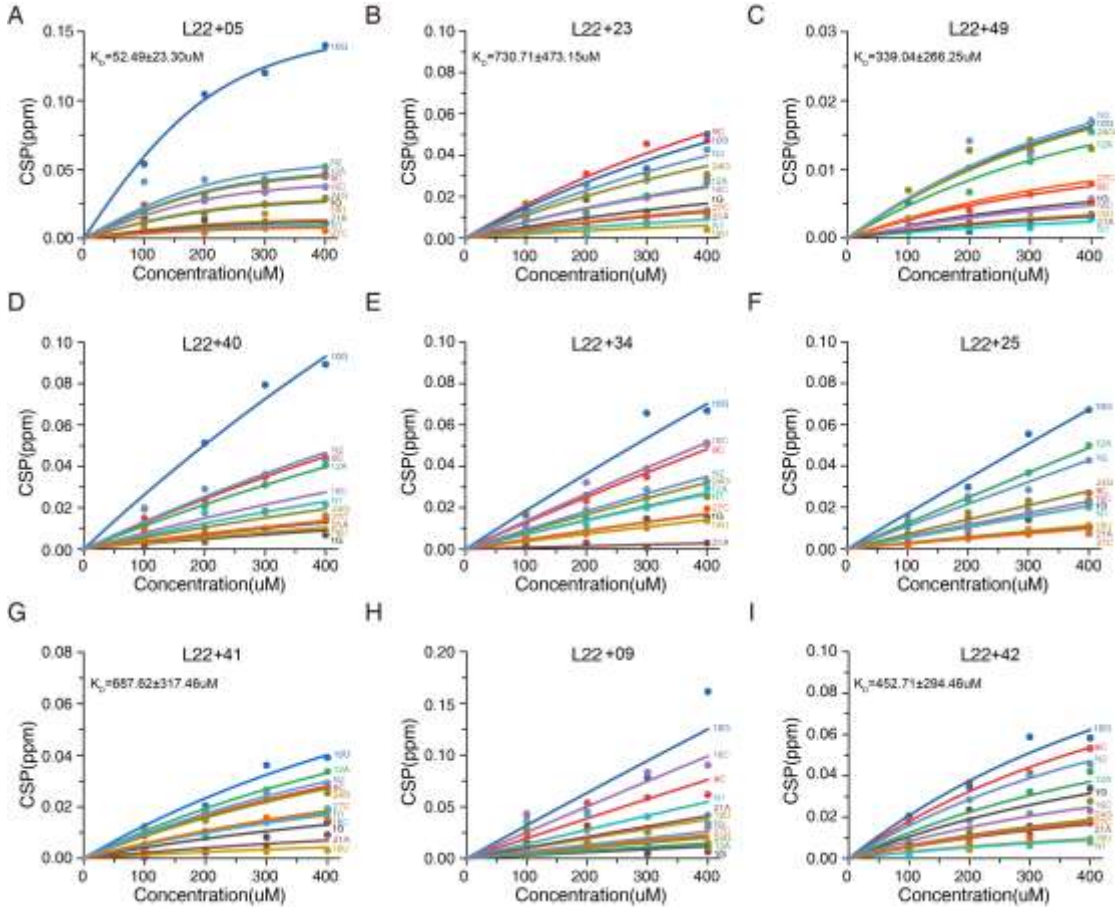

Figure S17. Global fitting of the binding equilibrium constant of the other 9 peptides to RBE RNA using nucleotides exhibiting significant CSPs (represented by different colors).